STUDY OF SUSPENDED SEDIMENT DISTRIBUTION USING NUMERICAL MODEL AND SATELLITE DATA IN BENOA BAY-BALI, INDONESIA

I Gede Hendrawan and Koji Asai

Abstract. The distribution of suspended sediment and its concentration within Benoa bay was calculated by a numerical model and utilization of satellite data. A two-dimensional coupled hydrody nam ic- transport model for the distribution characteristics of suspended sediment within the bay is presented here. Three-river discharges and sewerage installation outlets were used as source points of the suspended sediment. The model result showing the distribution of suspended sediment pattern follows the tidal level dynamic. It is concerned to the current pattern generated by tidal. The ALOS/AVNIR'2 satellite data also have good capability to investigate the suspended sediment distribution in coastal area. By using visible channels and developed regression of Digital Number (DNs) of AVNIR-2 data and observation data, the distribution of suspended sediment in Benoa bay was generated. Numerical model and satellite data quantitatively have the same tendency, but slightly different value. It is because of die differences in pollutant sources point.

Keywords: Numerical model, satellite data, suspended sediment

1. Introduction

Suspended sediments arc the most common pollutant both in term of weight and volume in surface water. Suspended sediments may serve many of contaminant from agriculture activity in watershed or upland area and discharge to the coaslal area by river transport.

The calculation of particulate movement in coastal area and representation of the processes involved in suspended solid transport, for use in mathematical tidal model and remote sensing technique, is a challenging objective. Many estuarine, lake and river waters have significant water quality problems which are often related to fine-grained sediment that has a harmful effect on the ecosystem, often carrying contaminants and reducing light needed for primary production. Better prediction of sediment transport, and redistribution is of great importance for integrated water and ecosystem management. Sediment transport models have been applied to engineering problems and *Lee el a/.* (2007) successfully applied two-dimensional sediment transport model that showed capable of simulating sediment resuspension of mixed (cohesive plus noncohesive) sediment. Clarke and Elliot (1998) presented 2D depth-integrated sediment transport model to study the resuspension and movement of sediment in the lower estuary. These transport models were forced by varying current systems in the study area, which is induced by hydrodynamic model.

Department of Civil and Environmental Engineering, Yamaguchi University (2-16-1 Tokiwadai, Ube,Yamaguchi 755-8611.Japan)

Beside a numerical model, in recent year satellite data utilizations are also significantly increasing in order to monitor coastal environment. The large areal coverage of remotely sensed satellite image makes them useful for mapping and monitoring large regions and studying large ecosystem. This can be important in helping to understand how various part of an ecosystem are reacting to environmental stress introduced at different locations and/or to climatic differences that occurred temporally and spatially.

Satellite remote sensing provides reliable quantified data on the concentration of the suspended matter in water. The satellite image also can provide key data for calibration, refining and validation of the numerical sediment-transport model elaborated. Kouts *et al.* (2007) presented sediment monitoring using MODIS satellite data and combine with numerical model. Booth *et al. (2000)* combined wind-driven resuspension model with AVHRR imagery to characterize sediment resuspension.

In the present study was aimed at the development of monitoring suspended sediment concentration and its distribution using a combination of advection-diffusion model and the satellite data within Benoa Bay.

2. The study area

Benoa bay is located in southern part of Bali Island, Indonesia. The bay is 8 km in length and 6 km in width. The average water depth is about 5 m with the deepest area in bay mouth about 48 m. The area surrounding Benoa bay developed rapidly, as an urban area and as tourism destination. Benoa bay is the main harbor in Bali Island of International and regional transportations.

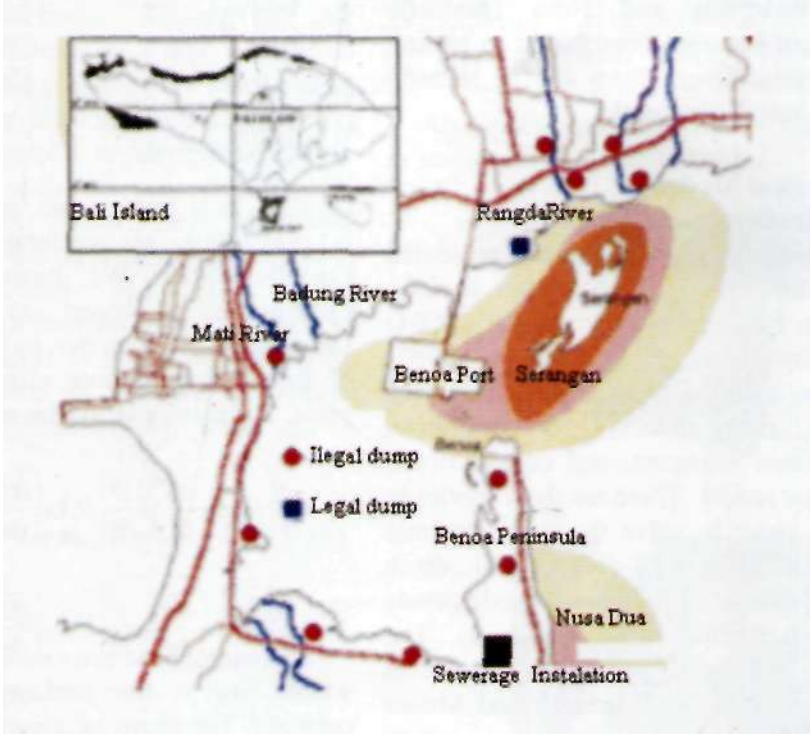

Figure 1. Benoa Bay map

Benoa Bay area has an important role for coastal ecosystem in the Sothern part of Bali island. Surrounding the bay edge, there is die largest area of mangrove habitat in Bali, namely Taman Hutan Raya (TAHURA). Japan International Cooperation Agency (JICA) gave some support to maintain the ecosystem in Benoa Bay. There are three main rivers: Mati river, Badung river, and Rangda river discharging of fresh water to the bay. There is also a legal garbage dump and some illegal garbage dump that decreases water quality. In Southern part of bay is Benoa peninsula and Nusa Dua, which is the place for tourism accommodation services in Bah, such as hotels and restaurants. A wastewater installation was established in the south side of Benoa Bay. It is concerned in overcoming the problem of wastewater from tourism activity in Benoa Peninsula and Nusa Dua. Its installation has also contributed to adding suspended sediment from sludge flowing out from installation outlet.

3. Numerical Model

3.1. Hydrodynamic Model

The basic equations here are presented for two-dimensional depth average velocity based on Princeton Ocean Model (POM) created by Blumberg and Mellor (1987) POM is a three-dimensional, primitive equation, time-dependent, *a* coordinate, free surface, estuarine, and coastal ocean circulation model. There are three modes in POM in order to solve the hydrodynamic model, which are 2-dimensional depth averaged (mode 2), prognostic mode (mode 3) and diagnostic mode (mode 4). The equation, which is used for this research, are presented as by Blumberg and Mellor (1987) as follows:

$$\frac{\partial \eta}{\partial t} + \frac{\partial \bar{U} D}{\partial x} + \frac{\partial \bar{V} D}{\partial y} = 0 \qquad (1)$$

$$\frac{\partial \bar{U} D}{\partial t} + \frac{\partial \bar{U}^2 D}{\partial x} + \frac{\partial \bar{U}\bar{V} D}{\partial y} - \tilde{F}_x - f\bar{V}D + gD\frac{\partial \eta}{\partial x} = -\langle wu(0)\rangle + \langle wu(-1)\rangle \qquad (2)$$

$$\frac{\partial \bar{V} D}{\partial t} + \frac{\partial \bar{U}\bar{V} D}{\partial x} + \frac{\partial \bar{V}^2 D}{\partial y} - \tilde{F}_y + f\bar{U}D + gD\frac{\partial \eta}{\partial x} = -\langle wv(0)\rangle + \langle wv(-1)\rangle \qquad (3)$$

Equations (1), (2), and (3) are continuity equations and momentum equations respectively, where: D = *H* + TJ; *U*, *V* are component of depth averaged velocity for *-axis and y-axis, respectively, and calculated as follows;

$$\bar{U} = \frac{1}{D}\int_{-1}^{0} U \, d\sigma \qquad (4)$$

and

$$\bar{V} = \frac{1}{D}\int_{-1}^{0} V \, d\sigma \qquad (5)$$

t is time, *H* is water depth, *rj* is elevation, *g* is gravitation at acceleration and / is Coriolis effect. We have ignored the Coriolis effect based on the Rossby Deformation Radius due to the small scale of Benoa Bay without effect on Coriolis force. Diffusivity terms are as follow:

$$\tilde{F}_x = \frac{\partial}{\partial x}\left[H2\bar{A}_M \frac{\partial \bar{U}}{\partial x}\right] + \frac{\partial}{\partial y}\left[H\bar{A}_M\left(\frac{\partial \bar{U}}{\partial y} + \frac{\partial \bar{V}}{\partial x}\right)\right] \qquad (6)$$

$$\tilde{F}_y = \frac{\partial}{\partial y}\left[H2\bar{A}_M \frac{\partial \bar{V}}{\partial y}\right] + \frac{\partial}{\partial x}\left[H\bar{A}_M\left(\frac{\partial \bar{U}}{\partial y} + \frac{\partial \bar{V}}{\partial x}\right)\right] \qquad (7)$$

where: *AM* is the horizontal diffusivity constant. The terms of <*wu(0)*> and <*wu(-l)*> are wind friction and bottom friction, respectively.

In order to obtain the values *U* and V and *t]*, boundary condition was considered. For open boundary condition has been used Orlanski radiation. And for closed boundary condition *(U.V.rf) = 0. Courant-Friedrich-Levy* (CFL) was used for the computational stabilization. The initial condition for velocity component of *U* and *V* are zero.

3.2. Mass **Transport Model**

In the mass transport model, it has been applied to two-dimensional advection-diffusion horizontal model proposed by Rivera[6] as follows:

$$\frac{\partial C}{\partial t} + \bar{U}\frac{\partial C}{\partial x} + \bar{V}\frac{\partial C}{\partial y} = K_x\frac{\partial^2 C}{\partial x^2} + K_y\frac{\partial^2 C}{\partial y^2} + \frac{\varphi_r - \varphi_s}{D} \quad (8)$$

C is sediment concentration, *U* and V are depth averaged flow velocities in *x* and v direction respectively, K_x and K_y are diffusion coefficients in *x* and y direction respectively, and $<p_r$ and $<p_s$ are erosion term and deposition term respectively. In left hand side equation is termed advection processes, its sediment concentration will be moved by water flow direction. Meanwhile in the right hand side equation is diffusion and source-sink term.

Treatment of erosion and deposition in sediment transport is important for study. The erosion term is function of bottom shear stress r_b and critical stress r_{cr} as follow:

If $\tau_b > \tau_{cr}$, then

$$Sources:\ \varphi_r = k_r \exp\{\alpha(\tau_b - \tau_{cr})^{0.5}\} \quad (9)$$

If $\tau_b < \tau_{cr}$, then

$$Sources:\ \varphi_r = 0$$

And for deposition term is as follow:

If $C^n_{i,j} > C_0$, then

$$Sink:\ \varphi_s = W_s(C^n_{i,j} - C_o) \quad (10)$$

If $C^n_{i,j} < C_0$, then

$$Sink\ \varphi_s = 0$$

k_r, a, C_0, and W_s are resuspension coefficient, resuspension parameter, threshold concentration and settling velocity respectively.

4. Satellite Data Processing

Remote sensing data that can be uses in the analysis of sediment transport are various and available in many countries, one of have capability is Advance Land Observing satellite (ALOS) with Advance Visible and Near-Infrared Radiometer type-2 (AVNIR-2). AVNIR-2 is a visible and near infrared radiometer for observing land and coastal zones. It has launched by Japan Aerospace Exploration Agency (JAXA) in January 2006. Its Japanese name is "DAICHI". AVNIR-2 has 4 bands with characteristic as shown as follows:

Table 1. ALPS/AVNIR-2 characteristic

Spectral Band	Bandwidth
Bandl	0.42 - 0.50
Band 2	0.52-0.60
Band 3	0.61-0.69
Band 4	0.76-0.89

The spatial resolution of AVNIR-2 is 10 m and with swath width 70 km.

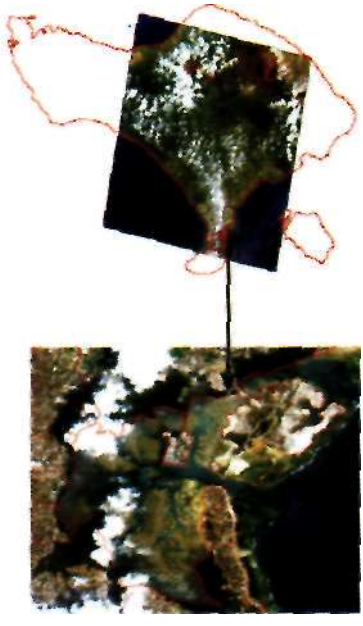

Figure 2. AVNIR-2 satellite data in Benoa Bay.

In general, the reflectance of water increases with increased suspended sediment concentration. One of the goals in this point used satellite data is to developed algorithm by converted of digital number (DNs) by in-situ data. The visible wavelength images were used for suspended sediment calculation. It corresponding to ability of visible channel in penetrates of water column Natesan[5].

In order to produce suspended sediment distribution within Benoa bay, DNs of satellite data was converted to physical value using regression analysis. The satellite image DNs and the water parameter value were used as input to made regression analysis. The regression was found as shown bellow:

$$TSS = -1.315bl+2.371b2-0.791b3+9.649 \quad (11)$$

b1, b2, and b3 are DNs of band 1, band2 and band3 of AVNIR-2 respectively with coefficient determination r^2 was 0.859. The AVNIR-2 data to be calculated is shown in Figure 2.

5. Result and Discussion

5.1. Current system

The hydrodynamic model was run for 30 days. The tidal input in open boundary condition was used tidal data prediction that developed by Ocean Research Institute (ORI) The University of Tokyo, namely ORITIDE. For the numerical simulation, the horizontal grid was rectangular with size are $Ax = Ay = 125$ m. The time step in considering the CFL stabilization. *At,* was used 2 second.

In order to test our model the tidal level data prediction in Benoa bay tidal gauge station was compared with numerical simulation as shown in Figure 3. It's shown that the simulation result gives a good agreement with tidal data in Benoa tidal station. The tidal pattern and tidal amplitude presented the same patterns. It means this model was simulated well for tidal level.

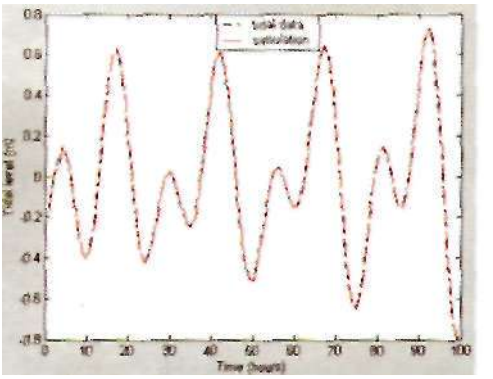

Figure 3. Tidal verification.

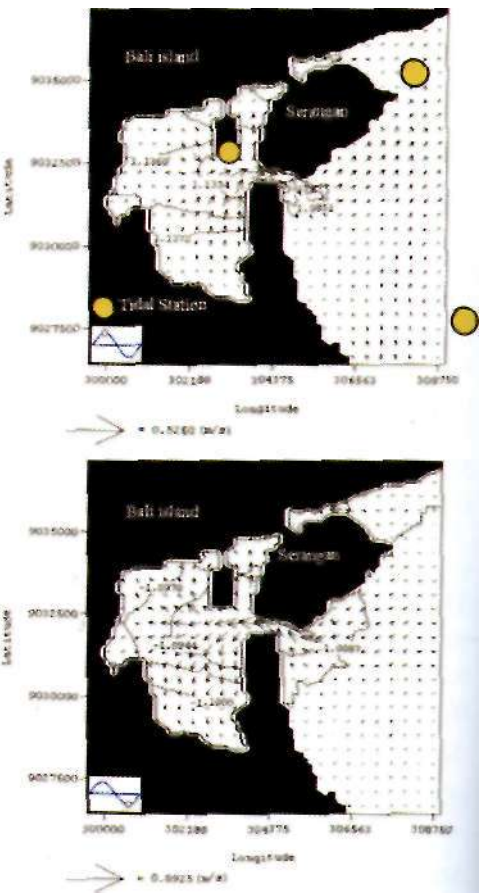

Figure 4. Tidal current pattern and elevation during ebb tide *(upper)* and flood tide *(below)* during spring tide imposed with tidal level.

Figure 4 shows a representative snapshot of the depth average tidal current

by POM during spring tide. It clearly illustrates the tidal exchange in the bay mouth indicating tidal forces have high sensitivity to tidal current within the bay.

The highest velocity occurred in the area surrounding the bay mouth, resulting the narrowed of its channel. The result for the highest velocity field during ebb tide and flood tide are 0.528 m/s and 0.892 m/s respectively.

5.2. Suspended Sediment Distribution by Numerical Model

The distribution of suspended sediment (SS) concentration in two-dimensions is described by equation (8) which includes both advection and diffusion. This model was assumed that the source of SS only came from three river discharge and sludge from the sewerage installation in Nusa Dua (south side of the bay). Based on observation of SS at in each source point, it was used for the initial condition for SS distribution within the bay. The in-situ data that used in this model was taken at 0.2 of water depth in order to represent the whole vertical pollutant distribution within the bay. SS also assumed pollutant continuation but the water flow rate from three rivers was low, so in this model are neglected.

Figure 5 shows the distribution of suspended sediment within the bay generated by a numerical model. A high concentration was shown surrounding each river discharge and sewerage installation outlet. At the peak of flood tide, the distribution of SS is converge entering the bay, otherwise at the peak of ebb tide, the SS distribution was dispersed within the bay. The high and low SS concentration was caused by the tidal current velocity fluctuation.

Figure 6 shows the variability of SS with the tidal level. It is shown that the curve has an opposite direction. When the tidal level is high the SS becomes low, and becomes high, as tidal level lowers. It does occur since during flood tide, water is flowing entering the bay. So that SS from source will be retained to the nearest source point and converge within the bay. And during ebb tide, seawater is flowing out from the bay, and at that time SS is also transported following the water direction to be disperse of SS (advection effect).

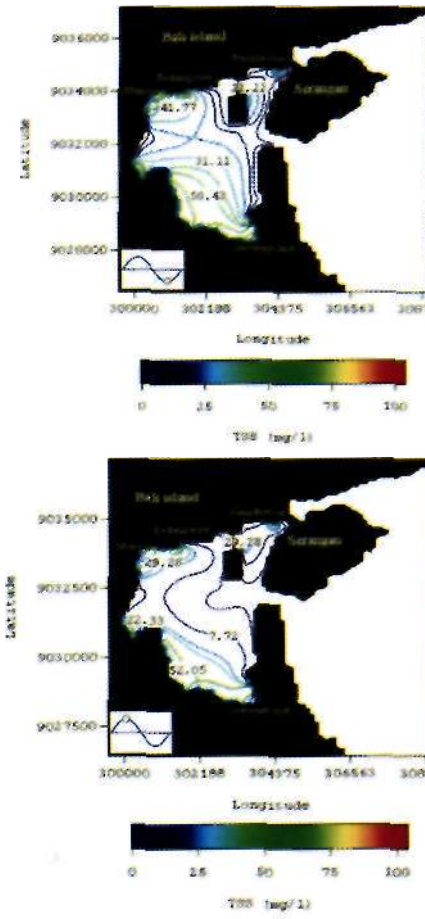

Figure 5. Suspended sediment distribution by Numerical Model.

The movement of SS within North side, south side and bay mouth is shown in Figure 7. In the north side, SS varies with small range compared to the south side. It occurred related to flow velocity that in north side was blocked by Benoa port. In bay mouth the variability of SS

concentration was smaller than inside of bay, this correlated with the higher velocity surrounding the bay mouth.

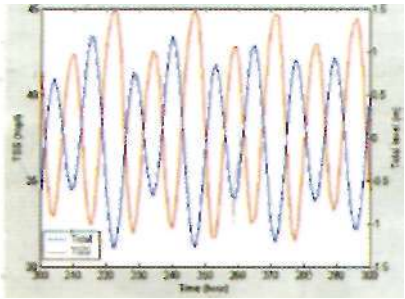

Figure 6. Variability of SS by tidal level

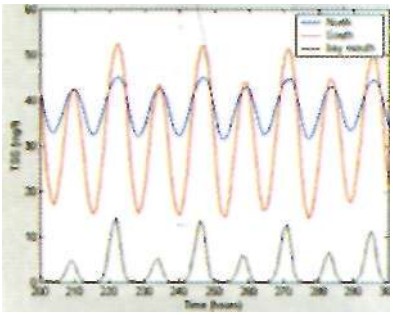

Figure 7. SS variability in north side, south side and bay mouth.

5.3. Suspended Sediment distribution by Satellite data

ALOS-Avnir-2 data was used to characterize the spatial distribution of the suspended sediment in Benoa Bay. The data was geometrically rectified fo a longitude-latitude coordinate system using header data imbedded in the original data. In order to reduce the atmospheric bias, radiometric correction was done using histogram adjustment approach.

Figure 8 shows the SS distribution of AVNIR-2 data using equation (7). Note that the non-water pixels have been set to zero and show up as black in the images. The image result showed that the higher SS concentration occurred in south part of the bay, and relatively high surrounding northern part of the bay. The SS concentration is also high surrounding behind the Serangan Island, since it is caused by the island reclamation that had brought many of the SS material. Otherwise a low level of SS concentration was found in the bay mouth and outside (open ocean) of the bay, most of its location is in the deeper channel.

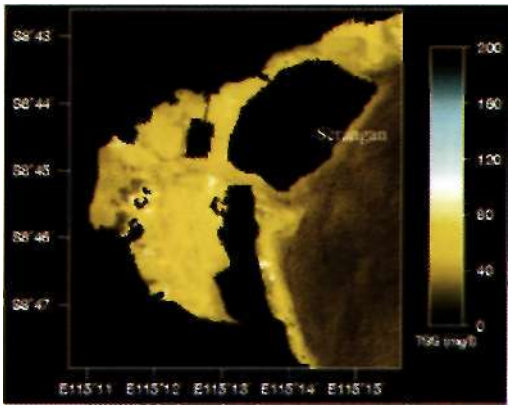

Figure 8. SS by AVNIR-2 data

6. Comparison of Numerical Model and Satellite Data of SS Distribution

The spatial distributions of SS were calculated by both numerical model and satellite data discussed in previous section. In general, the spatial distribution of SS has same patterns among the data results.

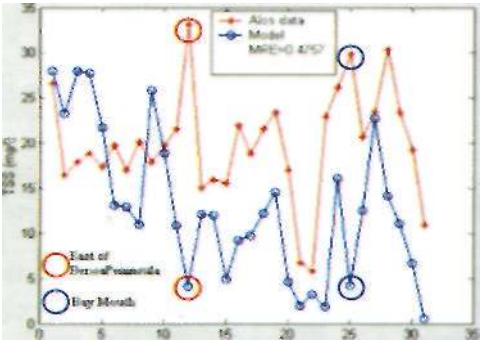

Figure 9. Comparison of SS concentration among Numerical Model and Satellite data

Figure 9 shows the comparison of SS between the numerical model and the satellite data in some sample point inside the bay. It is shown that the SS relatively has a same tendency, but with a slightly

different level among both of method. The difference value between the satellite data and the model in the eastern part of Benoa Peninsula and bay mouth is correlated with the SS transport from the open ocean to the bay that included in calculation using the satellite data. In order to know the difference level of SS between numerical model and satellite data, the mean relative error (MRE) was calculated. The MRE value of numerical model to the remote sensing result was 0.4757. The difference of SS concentration between the numerical model and the satellite data was occurred since sources of SS in model only accommodate from river discharge and sewerage installation outlet. The other way SS sources of satellite data was from all sources point such as Open Ocean, material from reclamation of island, etc.

7. Conclusion

The spatial distribution of SS in Benoa bay was modeled using a Hydrodynamic-transport equation model. The Model result showed the SS distribution surrounding the source point, and also varying during tidal level. This result has same pattern with SS distribution by satellite data. Except surrounding behind of Serangan Island, since affected by reclamation of its island.

Numerical model and satellite data have good capability to investigate the distribution of SS. Even so, these methods still have some weaknesses. Visible channel of satellite sensor can detect only the surface information of SS, we get in deep water will got high gap information for the SS concentration.

In the future investigation, the more observed data is needed in order to verify of model and satellite data become precisely.

Anknowledgment

The satellite ALOS-AVNIR-2 data was obtained by Centre for Remote Sensing and Ocean Sciences, Udayana University-Bali.

References

Blumberg, A. F. and G. L. Mel lor, 1987, A Description of a three dimensional coastal ocean circulation model. In Three-Dimensional Coastal Ocean Model, Coastal Estuarine Studies, American Geophysical Union (4): 1-16.

Booth, J. G., R. L. Miller, B. A. McKee, and R. A. Leathers, 2000, Wind-induced bottom sediment resuspension in a microtidal coastal environment, Continental Shelf Research 20:785-806.

Clarke, S. and A. J. Elliot, 1998, Modeling suspended sediment concentration. The Forth of Forth, Estuarine, Coastal and Self Science 47:235-250.

Kouts, T, S. Liis, S. Natalja, and R. Urmas, 2007, Environmental monitoring of water quality in Coastal Sea Area Using Remote Sensing and Modeling, Environmental Research, Engineering and Management 1(39): 8-13.

Lee, C. et al., 2007, Numerical modeling of mixed sediment resuspension, transport, and deposition during the March 1998 episodic events in southern Lake Michigan, Journal of Geophysical Research 112.

Rivera, R C, 1997, Hydrodynamics, sediment transport and light extinction of Cape Bolinao, Philipines, The Wageningen Agriculture University, Thesis for Doctoral Degree, Balkena Rotterdam, TheNederlands.